Influence of Size Factors in the Electroluminescent Emission of Large Area GaAs IRED's

Rosa F. Reyna, Antonio Martí, Carlos Algora, Juan C. Maroto, and Gerardo L. Araújo

Abstract—**A model to explain the current dependence of the external quantum efficiency of GaAs LED's is presented. First, this efficiency increases with the current due to the relative increase of the diffusion current in the total current; then, it remains constant since the diffusion current becomes dominant and finally, decreases due to series resistance effects, in absence of thermal effects.**

I. INTRODUCTION

It has been reported in some papers that, in practical GaAs infrared emitting diodes (IRED's), the external quantum efficiency first increases, reaches a maximum and then decreases with the injected current [1]–[3]. Also, it has been reported [4]–[6] that there is a sublinear characteristic of light intensity (equivalent to a drop in efficiency) as a function of current, at high currents. One of the references [4] explains that the drop in efficiency is due to thermal effects, and others [1], [2], [6] attribute the drop not only to thermal effects but also to the influence of series resistance effects. Another paper [7] presents an analysis for the external quantum efficiency at low currents. However, these papers do not include an explicit model of the external quantum efficiency, as a function of the current density, that shows the influence of series resistance effects on the efficiency. The purpose of this paper is to deduce such an expression and explain our experimental results on the basis of the derived theory.

II. THEORETICAL MODEL

To carry out the analysis we consider the device as a parallel interconnection of rectangular unit cells, periodically spaced in the x direction by $2S$. We also restrict the analysis to a simplified structure consisting of an emitter and a base region. We assume that the current flows horizontally (in the x direction) in the emitter and vertically (in the z direction) across the junction and in the base. When the current flows in the emitter, there is a voltage gradient in this region depending on x due to the presence of the emitter lateral resistance. Therefore, we assume that the currents in the emitter, in the base and across the junction are only functions of x. Then, the current density that flows across the junction takes the form

$$J_B(x) = J_{02} \exp \frac{V_j(x)}{2V_t} + J_{01} \exp \frac{V_j(x)}{V_t} \tag{1}$$

where $V_j(x)$ represents the voltage drop across the junction and $V_t = kT/q$. The first component represents the nonradiative recombination current in the space charge region and the second one, the recombination current in the neutral regions that is mainly radiative. For low injection, currents in the emitter and base neutral regions cause a voltage drop that can be determined by Ohm's law. The current density in the emitter and the x-dependence of the voltage

Manuscript received May 2, 1996; revised January 8, 1997. The review of this brief was arranged by Editor P. K. Bhattacharya.

The authors are with Departamento Electrónica Fìsica, E.T.S.I.T., Ciudad Universitaria s/n, 28040 Madrid, Spain.

Publisher Item Identifier S 0018-9383(97)04684-4.

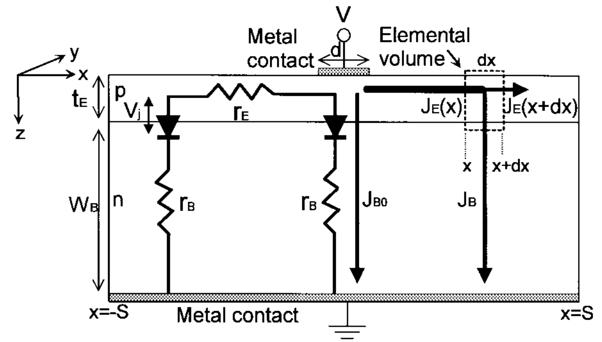

Fig. 1. Cross section of one of the elemental units that constitutes the IRED. On the right, our assumption as to how the current density flows through the device is shown. Also shown is the elemental volume that is used to solve the current continuity equation. On the left, an equivalent circuit is sketched, the units of r_i being $\Omega \cdot \mathrm{cm}^2$, and V_j the voltage drop in the junction.

distribution in the device take the form

$$J_B = -\frac{1}{\rho_B}\frac{dV_B}{dx} \quad V_j(x) = V_B(x) - r_b J_B(x) \tag{2}$$

where V_E is the voltage in the emitter referred to ground, ρ_E the emitter resistivity and $r_b = \rho_B W_B$, ρ_B being the base resistivity. The current continuity equation applied to an elemental volume as the one showed in Fig. 1 is

$$\frac{dJ_B}{dx} = -\frac{J_B}{t_B} \quad \frac{d^2V_B(x)}{dx^2} - R_B J_B(x) = 0 \tag{3}$$

where $R_E = \rho_E/t_E$ is the emitter sheet resistivity. The boundary conditions necessary to solve the equation above are $V_E(0) = V$ and $dV_E/dx(S) = 0$, which reflect the fact that a voltage V has been applied to the emitter metal electrode and the fact that, by symmetry considerations, there is no current flow through the plane $x = S$.

The unit cell may also be considered as a parallel interconnection of two diodes: one under the metal and another under the uncovered region. The considerations above refer to the last diode. The current density under the metal electrode is assumed constant with x and given by $J_{B0} = J_B(0)$. So the current injected is

$$I = A_M J_{B0} + \iint_{A_g} J_B(x)\, dx\, dy \tag{4}$$

J_{B0} can be an initial given excitation condition or calculated from (1) and (2), for $x = 0$, if the given initial variable is V. A_M represents the area covered by the metal electrode and A_E the uncovered area and therefore, the area through which the external emission of light is possible. The integral of (4) allows one to define an average emitter current, J_A. If equation (4) is divided by the total device area, A, we can write $J = F_M J_{B0} + (1 - F_M) J_A$, where $F_M = A_M/A$ and represents the fraction of the area covered by the metal.

The set of (1)–(3) has been extensively studied in [8] and its general solution, valid for our case study, can be found there. We reproduce here this solution adapted to our present notation and sign conventions. The solution consists of a) An expression for J_A [8, Eq. (9)]

$$J_A = J_{B0}\left[\frac{r_b}{r_e}\left(1 - \frac{J_{\mathrm{BS}}^2}{J_{B0}^2}\right) + \frac{2V_t}{r_e J_{B0}}\left(1 - \frac{J_{\mathrm{BS}}}{J_{B0}}\right)\right]^{1/2} \tag{5}$$

0018–9383/97$10.00 © 1997 IEEE

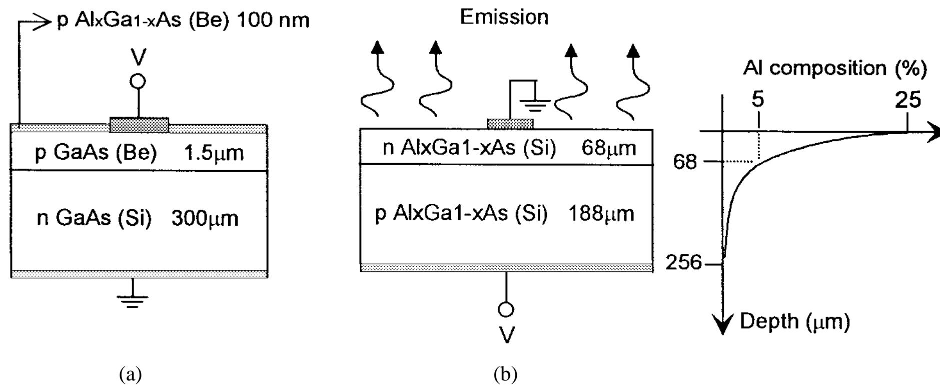

Fig. 2. Structures of the fabricated diodes: (a) GaAs homojunction and (b) $Al_xGa_{1-x}As$ heterojunction.

TABLE I
PARAMETERS OF THE FABRICATED DIODES

Diode	K(%)	F_M	J_{01} (A/cm^2)	J_{02} (A/cm^2)	A(cm^2)	d(μm)	R_E(Ω/□)	r_e(Ω cm^2)	r_b(Ω cm^2)
2J45	0.92	0.09	1.3 10^{-19}	5.3 10^{-11}	0.11	10	182.7	3.7 10^{-3}	5.2 10^{-5}
4J45	0.88	0.09	1.3 10^{-19}	5.3 10^{-11}	0.11	10	182.7	3.7 10^{-3}	5.2 10^{-5}
R46-1	6.0	0.09	3.0 10^{-20}	7.0 10^{-11}	0.11	10	55.4	1.4 10^{-3}	1.1 10^{-5}
R49-7	3.0	0.15	3.0 10^{-20}	7.0 10^{-11}	0.01	10	55.4	4.4 10^{-4}	1.1 10^{-5}

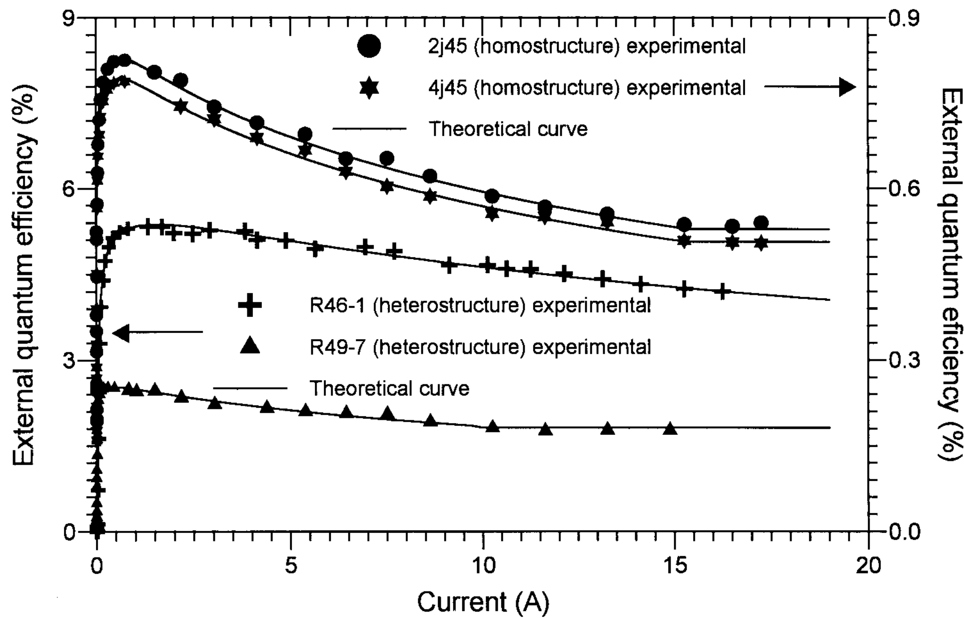

Fig. 3. Current dependence of the external quantum efficiency, theoretical (solid line) and experimental (symbols). The scale in the y-axis at the left is for the diodes with the structure shown in Fig. 2(b) and the scale in the y-axis at the right is for the diodes with the structure shown in Fig. 2(a).

where $J_{\rm BS} = J_B(S)$ and $r_e = R_E S^2$, and b) A relationship to calculate $J_{\rm BS}$ as a function of J_{B0} [8, Eq. (B3)]

$$V_t\left[J_{\rm BS}\left(\frac{r_b}{2}J_{\rm BS} - V_t\right)\right]^{-1/2} \cdot \cos^{-1}\left[\frac{J_{\rm BS}}{J_{\rm BO}} - \left(1 - \frac{J_{\rm BS}}{J_{\rm BO}}\right)\frac{V_t}{V_t - r_b J_{\rm BS}}\right] + (2r_b)^{1/2} \cdot \cosh^{-1}\left(\frac{V_t - r_b J_{\rm BO}}{V_t - r_b J_{\rm BS}}\right) = (2r_e)^{1/2}. \tag{6}$$

It will be assumed that only the diffusion component of the total current flowing under the uncovered area is effective for radiant emission. This allows us to write the light intensity $I_{\rm ph}$ and the external quantum efficiency as

$$I_{ph} = K\iint_{A_E} J_{01}\exp\frac{V_j(x)}{V_t}\,dx\,dy$$

$$\eta_{\rm ext}(J) \equiv \frac{I_{ph}}{I} = \frac{K}{AJ}\iint_{A_E} J_{01}\exp\frac{V_j(x)}{V_t}\,dx\,dy \tag{7}$$

where K is a proportionality constant.

The study has been carried out into different ranges of current in order to simplify (1), (5), and (6) and determine the analytical expressions for the external quantum efficiency (7) in each of these ranges.

1) Region I (Low Currents): In this case, the series resistance effects do not show up and therefore, there is a uniform distribution of the current. Hence, all the z-current components are constant and equal and given by $J_{B0} = J_A = J = I/A$. The resulting expression for $\eta_{\text{ext}}(J)$ is obtained from (1) and (7)

$$\eta_{\text{ext,I}}(J) = K(1 - F_M)\left[1 - \frac{J_{02}^2}{2J_{01}}\left(\sqrt{1 + \frac{4J_{01}J}{J_{02}^2}} - 1\right)\right]. \quad (8)$$

2) Region II (Medium Currents): At high enough currents, one may consider the space charge recombination current negligible compared to the diffusion current and the external quantum efficiency tends to $\eta_{\text{ext,II}}(J) = K(1 - F_M)$.

3) Region III-A (High Currents): In the third region, where the series resistance, or non uniform distribution of the current effects begin, for the common situation in which $r_e \gg r_b$ and for current densities greater than $2V_t/r_e$, (5) and (6) can be approximated to give

$$J_A = \sqrt{J_{B0}\frac{2V_t}{r_e}}. \quad (9)$$

If we assume again that the space charge recombination current is negligible then the external quantum efficiency can be expressed as

$$\begin{aligned} \eta_{\text{ext,IIIA}}(J) &= \frac{K}{AJ}\iint_{A_E} J_B(x)\,dx\,dy = K(1 - F_M)\frac{J_A}{J} \\ &= K\frac{(1 - F_M)^2}{F_M}\frac{V_t}{Jr_e} \\ &\quad \cdot \left[\sqrt{1 + \frac{2F_M}{(1 - F_M)^2}\frac{Jr_e}{V_t}} - 1\right]. \end{aligned} \quad (10)$$

This expression predicts a decrease of the external quantum efficiency with an increase in current. The greater the value of r_e, the greater the decrease of the efficiency with current.

4) Region III-B (Very High Currents): The series resistance effects become more severe so that (5) and (6) can be approximated to give

$$J_A = J_{\text{BO}}\sqrt{\frac{r_b}{r_e}}\tanh\sqrt{\frac{r_e}{r_b}}. \quad (11)$$

Proceeding as before, the external quantum efficiency tends to stabilise at a minimum value given by

$$\begin{aligned} &\eta_{\text{ext,IIIB}}(J) \\ &= K(1 - F_M)\frac{\sqrt{\frac{r_b}{r_e}}\tanh\sqrt{\frac{r_e}{r_b}}}{F_M + (1 - F_M)\sqrt{\frac{r_b}{r_e}}\tanh\sqrt{\frac{r_e}{r_b}}}. \end{aligned} \quad (12)$$

III. Experimental

Two types of diodes have been fabricated. One of them presents the structure shown in Fig. 2(a). It consists of a p-n GaAs junction passivated with a p-$Al_xGa_{1-x}As$ layer. The two p-type layers are doped with beryllium and the substrate is doped with silicon. The other structure, whose wafer was kindly supplied by Sumitomo Ltd and processed in our laboratory, is the one showed in Fig. 2(b). It consists of an $Al_xGa_{1-x}As$ heterojunction doped with silicon in both the p-layer and n-layer. The details concerning device parameters can be found in Table I.

The total light output was measured by a calibrated large area photodiode. The injected current is continuous at low levels and pulsed (pulse width 1 μs, duty cycle 1%) at high currents to reduce device heating. Heating is also decreased by means of a good thermal contact achieved by soldering the devices onto a copper disk. The external quantum efficiency, measured as explained, is shown in Fig. 3 by symbols. The theoretical external quantum efficiency for these devices, obtained from the model, explained above, with the parameters given in Table I is plotted by solid lines. It can be observed that there is a satisfactory agreement between experiment and theory.

IV. Summary

We have obtained the functional forms for the current dependence upon the external quantum efficiency, in the different regions of the variation of the current. At low current values, the increase in efficiency with the current is explained by the presence of the space charge recombination current (fundamentally non radiative) in the total current. At high currents, the drop of the efficiency, that appears in absence of thermal effects, is explained by nonuniform distribution of the current (series resistance effects) throughout the device. The theoretical equations obtained present a good agreement with experimental data.

References

[1] K. Kurata, Y. Ono, K. Ito, M. Mori, and H. Sano, "An experimental study on improvement of performance for hemispherically shaped high-power IRED's with $Ga_{1-x}Al_xAs$-grown junctions," *IEEE Trans. Electron Devices*, vol. ED-28, pp. 374–379, Apr. 1981.

[2] A. M. Kontkiewicz, "The influence of design factors on the radiation power of GaAs:Si LED's," *Electron Technol.*, vol. 13, no. 4, pp. 81–96, 1982.

[3] S. V. Galginaitis, "Efficiency measurements on GaAs electroluminescent diodes," *J. Appl. Phys.*, vol. 35, no. 2, pp. 295–298, Feb. 1964.

[4] T. P. Lee and A. G. Dentai, "Design criteria for GaAs-AlGaAs high-radiance LED's for optical fiber communication systems," *IEEE Trans. Electron Devices*, vol. ED-33, p. 1254, Nov. 1976.

[5] Y. Ono, M. Mori, K. Ito, and K. Kurata, "High-power and high-speed characteristics of modified heterostructure IRED's," *IEEE Trans. Electron Devices*, vol. ED-28, pp. 1183–1187, Oct. 1981.

[6] W. N. Carr and G. E. Pittman, "One-watt GaAs p-n junction infrared source," *Appl. Phys. Lett.*, vol. 3, no. 10, pp. 173–175, Nov. 1963.

[7] Y. Tanaka and T. Toyama, "Analysis of current-temperature-light characteristics of GaAsP light-emitting diodes," *IEEE Trans. Electron Devices*, vol. 41, pp. 1475–1477, Aug. 1994.

[8] G. L. Araújo, A. Cuevas, and J. M. Ruiz, "The effect of distributed series resistance on the dark and illuminated current-voltage characteristics of solar cells," *IEEE Trans. Electron Devices*, vol. ED-33, pp. 391–401, Mar. 1986.